

COMPRESSIVE INVERSE SCATTERING II. SISO MEASUREMENTS

ALBERT C. FANNJIANG

ABSTRACT. Inverse scattering schemes based on the restricted isometry property (RIP) in compressed sensing are proposed and analyzed. The methods employ randomly and repeatedly (multiple-shot) the single-input-single-output (SISO) measurements in which the frequency, the chosen incidence and the sampling angle are related in a precise way and are capable of recovering exactly (point of extended) scatterers of sufficiently low sparsity. Two schemes are particularly interesting: The first one employs multiple frequencies with the sampling angle always in the back-scattering direction resembling the synthetic aperture (SA) imaging; the second employs only single frequency with the sampling angle in the (nearly) forward scattering direction in the high frequency limit, resembling that of the X-ray tomography.

1. INTRODUCTION

Consider the scattering of the incident plane wave

$$(1) \quad u^i(\mathbf{r}) = e^{i\omega \mathbf{r} \cdot \mathbf{d}}$$

by the variable refractive index $n^2(\mathbf{r}) = 1 + \nu(\mathbf{r})$ where \mathbf{d} is the incident direction. The scattered field satisfies the Lippmann-Schwinger equation [9]

$$(2) \quad u^s(\mathbf{r}) = \omega^2 \int_S \nu(\mathbf{r}') (u^i(\mathbf{r}') + u^s(\mathbf{r}')) G(\mathbf{r}, \mathbf{r}', \omega) d\mathbf{r}'$$

where $G(\mathbf{r}, \mathbf{r}', \omega)$ is the Green function of the operator $-(\Delta + \omega^2)$. We assume that the wave speed is unity and hence the frequency equals the wavenumber ω .

The scattered field has the far-field asymptotic

$$(3) \quad u^s(\mathbf{r}) = \frac{e^{i\omega|\mathbf{r}|}}{|\mathbf{r}|^{(d-1)/2}} (A(\hat{\mathbf{r}}, \mathbf{d}, \omega) + \mathcal{O}(|\mathbf{r}|^{-1})), \quad \hat{\mathbf{r}} = \mathbf{r}/|\mathbf{r}|, \quad d = 2, 3$$

where A is the scattering amplitude. In inverse scattering theory, the scattering amplitude is the measurement data determined by the formula [9]

$$(4) \quad A(\hat{\mathbf{r}}, \mathbf{d}, \omega) = \frac{\omega^2}{4\pi} \int d\mathbf{r}' \nu(\mathbf{r}') u(\mathbf{r}') e^{-i\omega \mathbf{r}' \cdot \hat{\mathbf{r}}}$$

The main objective of inverse scattering then is to reconstruct the medium inhomogeneities ν from the knowledge of the scattering amplitude. In Part I [13] and the present paper we study the inverse scattering problem using the compressed sensing techniques. In [13] we analyze the imaging method with the single-input-multiple-output (SIMO) measurements in which for every incident plane wave the scattering amplitude is measured at multiple sampling directions. In this paper we focus on the methods with the single-input-single-output (SISO) measurements in which for every incident plane wave the scattering amplitude is measured at only one sampling direction.

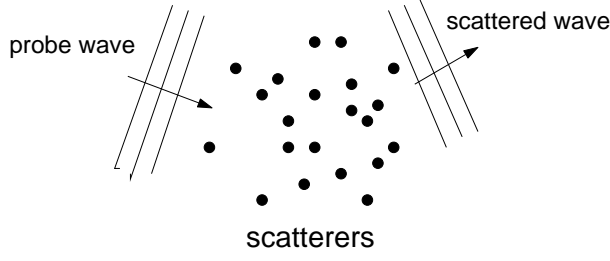


FIGURE 1. Far-field imaging geometry

As our approach is independent of the dimension we will focus on two dimensions below. We discuss the case with point scatterers in Section 2. We present the numerical results in Section 3 and conclude in Section 4.

2. POINT SCATTERERS

We consider the medium with point scatterers located in a square lattice $\mathcal{M} = \{\mathbf{x}_i = (x_i, z_i) : i = 1, \dots, m\}$ of spacing ℓ . The total number m of grid points in \mathcal{M} is a perfect square. Without loss of generality, assume $x_j = j_1\ell, z_j = j_2\ell$ where $j = (j_1 - 1)\sqrt{m} + j_2$ and $j_1, j_2 = 1, \dots, \sqrt{m}$. Let $\nu_j, j = 1, \dots, m$ be the strength of the scatterers. Let $\mathcal{S} = \{\mathbf{x}_{i_j} = (x_{i_j}, z_{i_j}) : j = 1, \dots, s\}$ be the locations of the scatterers. Hence $\nu_j = 0, \forall \mathbf{r}_j \notin \mathcal{S}$.

For the discrete medium the scattering amplitude becomes a finite sum

$$(5) \quad A(\hat{\mathbf{r}}, \mathbf{d}, \omega) = \frac{\omega^2}{4\pi} \sum_{j=1}^m \nu_j u(\mathbf{x}_j) e^{-i\omega \mathbf{x}_j \cdot \hat{\mathbf{r}}}.$$

Unlike [13] which covers both linear and nonlinear scattering, here we work exclusively under the Born approximation in which the exciting field $u(\mathbf{x}_j)$ is replaced by the incident field $u^i(\mathbf{x}_j)$; unlike [13] which deals exclusively with one frequency, here we will work with multiple frequencies.

Define the measurement vector $Y = (Y_l) \in \mathbb{C}^n$ with

$$(6) \quad Y_l = \frac{4\pi}{\omega^2} A(\hat{\mathbf{r}}_l, \mathbf{d}_l, \omega_l), \quad l = 1, \dots, n.$$

The measurement vector is related to the target vector $X = (\nu_j) \in \mathbb{C}^m$ by the sensing matrix \mathbf{A} as $Y = \mathbf{A}X$. Let $\theta_l, \tilde{\theta}_l$ be the polar angles of $\mathbf{d}_l, \hat{\mathbf{r}}_l$, respectively. The (l, j) -entry of $\mathbf{A} \in \mathbb{C}^{n \times m}$ is

$$(7) \quad e^{-i\omega_l(z_j \sin \tilde{\theta}_l + x_j \cos \tilde{\theta}_l)} u^i(\mathbf{x}_j) = e^{i\omega_l \ell (j_2 (\sin \theta_l - \sin \tilde{\theta}_l) + j_1 (\cos \theta_l - \cos \tilde{\theta}_l))}, \quad j = (j_1 - 1) + j_2.$$

As in [13] we reconstruct X as the solution of the L^1 -minimization, called Basis Pursuit (BP):

$$(8) \quad \min \|X\|_1 \quad \text{s.t. } \mathbf{A}X = Y$$

which can be solved by linear programming or by various greedy algorithms [2, 8, 10, 12].

A fundamental notion in compressed sensing under which BP yields the unique exact solution is the restrictive isometry property (RIP) due to Candès and Tao [6]. Precisely, let the sparsity s

of a vector $Z \in \mathbb{C}^m$ be the number of nonzero components of Z and define the restricted isometry constant δ_s to be the smallest positive number such that the inequality

$$(1 - \delta_s)\|Z\|_2^2 \leq \|\mathbf{A}Z\|_2^2 \leq (1 + \delta_s)\|Z\|_2^2$$

holds for all $Z \in \mathbb{C}^m$ of sparsity at most s . For the target vector X let X_s denote the best s -sparse approximation of X in the sense of L^1 -norm, i.e.

$$X^{(s)} = \operatorname{argmin} \|Z - X\|_1, \quad \text{s.t.} \quad \|Z\|_0 \leq s$$

where $\|Z\|_0$ denotes the number of nonzero components, called the sparsity, of Z . Clearly, $X^{(s)}$ consists of the s largest components of X .

Now we state the fundamental result of the RIP approach [3] which is an improvement of the results of [4, 6].

Proposition 1. [3] *Suppose the restricted isometry constant of \mathbf{A} satisfies the inequality*

$$(9) \quad \delta_{2s} < \sqrt{2} - 1$$

Then the solution \hat{X} by BP satisfies

$$(10) \quad \|\hat{X} - X\|_1 \leq C_0 \|X - X^{(s)}\|_1$$

$$(11) \quad \|\hat{X} - X\|_2 \leq C_0 s^{-1/2} \|X - X^{(s)}\|_1$$

for some constant C_0 . In particular, if X is s -sparse, then the recovery is exact.

We wish to write the (l, j) -entry of the sensing matrix in the form

$$(12) \quad e^{i\pi(j_1\xi_l + j_2\zeta_l)}, \quad j = (j_1 - 1)\sqrt{m} + j_2, \quad j_1, j_2 = 1, \dots, \sqrt{m}, \quad l = 1, \dots, n$$

where ξ_l, ζ_l are independently and uniformly distributed in $[-1, 1]$ in view of the following theorem.

Proposition 2. [16] *Suppose*

$$(13) \quad \frac{n}{\ln n} \geq C\delta^{-2}\sigma \ln^2 \sigma \ln m \ln \frac{1}{\alpha}, \quad \alpha \in (0, 1)$$

for a given sparsity σ where C is an absolute constant. Then the restricted isometry constant of the matrix with entry (12) satisfies

$$\delta_k \leq \delta$$

with probability at least $1 - \alpha$.

See [4, 7, 17] for the case when ξ_l, ζ_l belong to the discrete subset of $[-1, 1]$ of equal spacing $2/\sqrt{m}$.

To construct a sensing matrix of the form (12) we proceed as follows. Write (ξ_l, ζ_l) in the polar coordinates

$$(\xi_l, \zeta_l) = \rho_l(\cos \phi_l, \sin \phi_l), \quad \rho_l = \sqrt{\xi_l^2 + \zeta_l^2} \leq \sqrt{2}$$

and set

$$\begin{aligned} \omega_l(\cos \theta_l - \cos \tilde{\theta}_l) &= \sqrt{2}\rho_l\Omega \cos \phi_l \\ \omega_l(\sin \theta_l - \sin \tilde{\theta}_l) &= \sqrt{2}\rho_l\Omega \sin \phi_l \end{aligned}$$

where Ω is a parameter. Equivalently we have

$$(14) \quad -\sqrt{2}\omega_l \sin \frac{\theta_l - \tilde{\theta}_l}{2} \sin \frac{\theta_l + \tilde{\theta}_l}{2} = \Omega \rho_l \cos \phi_l$$

$$(15) \quad \sqrt{2}\omega_l \sin \frac{\theta_l - \tilde{\theta}_l}{2} \cos \frac{\theta_l + \tilde{\theta}_l}{2} = \Omega \rho_l \sin \phi_l.$$

This set of equations determines the single-input- (θ_l, ω_l) -single-output- $\tilde{\theta}_l$ mode of sampling.

The following implementation of (14)-(15) is natural. Let the sampling angle $\tilde{\theta}_l$ be related to the incidence angle θ_l via

$$(16) \quad \theta_l + \tilde{\theta}_l = 2\phi_l + \pi,$$

and set the frequency ω_l to be

$$(17) \quad \omega_l = \frac{\Omega \rho_l}{\sqrt{2} \sin \frac{\theta_l - \tilde{\theta}_l}{2}}.$$

Then the entries (7) of the sensing matrix \mathbf{A} have the form

$$(18) \quad e^{i\sqrt{2}\Omega \ell(j_1 \xi_l + j_2 \zeta_l)}, \quad l = 1, \dots, n, \quad j_1, j_2 = 1, \dots, \sqrt{m}.$$

By the square-symmetry of the problem, it is clear that the relation (16) can be generalized to

$$(19) \quad \theta_l + \tilde{\theta}_l = 2\phi_l + \eta\pi, \quad \eta \in \mathbb{Z},$$

Indeed, it will be seen below that any fixed $\eta \in \mathbb{R}$ produces essentially the same result.

Let us focus on three specific measurement schemes.

Scheme I. The first case is that of Ω -band limited signals, i.e. $\omega_l \in [-\Omega, \Omega]$. This and (17) lead to the constraint:

$$(20) \quad \left| \sin \frac{\theta_l - \tilde{\theta}_l}{2} \right| \geq \frac{\rho_l}{\sqrt{2}}.$$

The simplest way to satisfy (16) and (20) is to set

$$(21) \quad \phi_l = \tilde{\theta}_l = \theta_l + \pi,$$

$$(22) \quad \omega_l = \frac{\Omega \rho_l}{\sqrt{2}}$$

$l = 1, \dots, n$. In this case the scattering amplitude is always sampled in the back-scattering direction. This resembles the synthetic aperture imaging which has been previously analyzed under the paraxial approximation in [15]. In contrast, the forward scattering direction with $\tilde{\theta}_l = \theta_l$ almost surely violates the constraint (20).

Scheme II. The second case is that of single frequency no less than Ω :

$$(23) \quad \omega_l = \gamma \Omega, \quad \gamma \geq 1, \quad l = 1, \dots, n.$$

To satisfy (19) and (17) we set

$$(24) \quad \theta_l = \phi_l + \frac{\eta\pi}{2} + \arcsin \frac{\rho_l}{\gamma\sqrt{2}}$$

$$(25) \quad \tilde{\theta}_l = \phi_l + \frac{\eta\pi}{2} - \arcsin \frac{\rho_l}{\gamma\sqrt{2}}$$

with $\eta \in \mathbb{Z}$. The difference between the incidence angle and the sampling angle is

$$(26) \quad \theta_l - \tilde{\theta}_l = 2 \arcsin \frac{\rho_l}{\gamma\sqrt{2}}$$

which diminishes as $\gamma \rightarrow \infty$. In other words, in the high frequency limit, the sampling angle approaches the incidence angle. This resembles the setting of the X-ray tomography.

Scheme III. The third case is that of unlimited frequency band. Let θ_l be n arbitrary distinct numbers in $[-\pi, \pi]$ and let $\tilde{\theta}_l$ and ω_l be determined by (19) and (17), respectively. The possibility of having a small divisor in (17) renders the bandwidth unlimited in principle.

The following result is an immediate consequence of Proposition 1 and Proposition 2.

Theorem 1. *Let ξ_l, ζ_l be independently and uniformly distributed in $[-1, 1]$ and let (ρ_l, ϕ_l) be the polar coordinates of (ξ_l, ζ_l) , i.e.*

$$(\xi_l, \zeta_l) = \rho_l(\cos \phi_l, \sin \phi_l).$$

Let the probe frequencies ω_l , the incidence angles θ_l and the sampling angles $\tilde{\theta}_l$ satisfy (16) and (17), for example, by Scheme I, II or III.

Suppose

$$(27) \quad \Omega\ell = \pi/\sqrt{2}$$

and suppose (13) holds with $\sigma = 2s$ and any $\delta < \sqrt{2} - 1$. Then (9) is satisfied for the matrix \mathbf{A} with probability at least $1 - \alpha$ and the bounds (10)-(11) hold true. In particular, every target vector of sparsity less than s can be exactly recovered by BP.

Suppose the noise E is present in the measurement vector as described by

$$(28) \quad Y = \mathbf{A}X + E, \quad \|E\|_2 = \varepsilon > 0$$

and consider the relaxation scheme

$$(29) \quad \min \|Z\|_1, \quad \text{s.t.} \quad \|Y - \mathbf{A}Z\|_2 \leq \varepsilon.$$

The next result is a restatement of the result of [3] after applying Proposition 2 with $\sigma = 2s, \delta < \sqrt{2} - 1$.

Theorem 2. *Let \hat{X} be the solution to (29). Then under the assumptions of Theorem 1 we have*

$$(30) \quad \|\hat{X} - X\|_2 \leq C_0 s^{-1/2} \|X - X^{(s)}\|_1 + C_1 \varepsilon$$

with probability at least $1 - \alpha$ where C_0 and C_1 are constants.

3. NUMERICAL RESULTS

Greedy algorithms have significantly lower computational complexity than linear programming and have provable performance under various conditions. For example under the condition $\delta_{3s} < 0.06$ the Subspace Pursuit (SP) algorithm is guaranteed to exactly recover X via a finite number of iterations [10]. We have used SP for reconstruction in all our simulations with the following parameters: $m = 2500, \ell = 1, \Omega = \pi/\sqrt{2}, n = 100$. The probability of recovery is calculated by using 1000 independent runs.

To test Scheme I numerically, we use (22) and

$$(31) \quad \tilde{\theta}_l = \theta_l + \eta\pi, \quad \eta = 1, 1/2, 1/4, 1/8$$

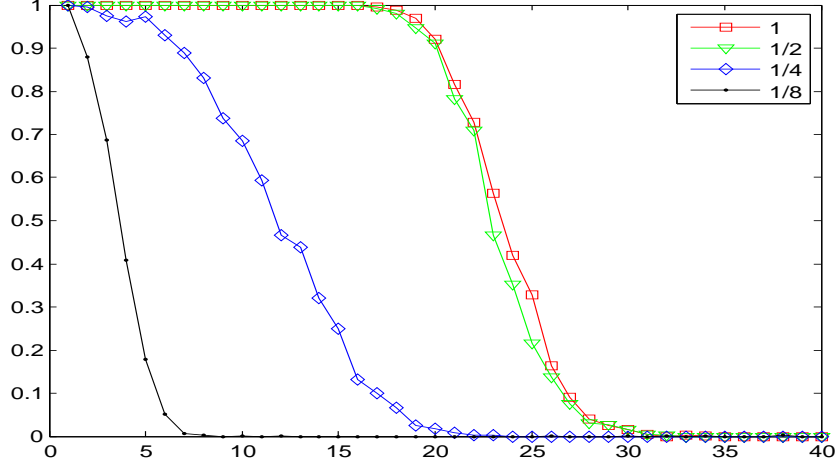


FIGURE 2. Success probabilities for Scheme I with (31). The label indicates the value of η .

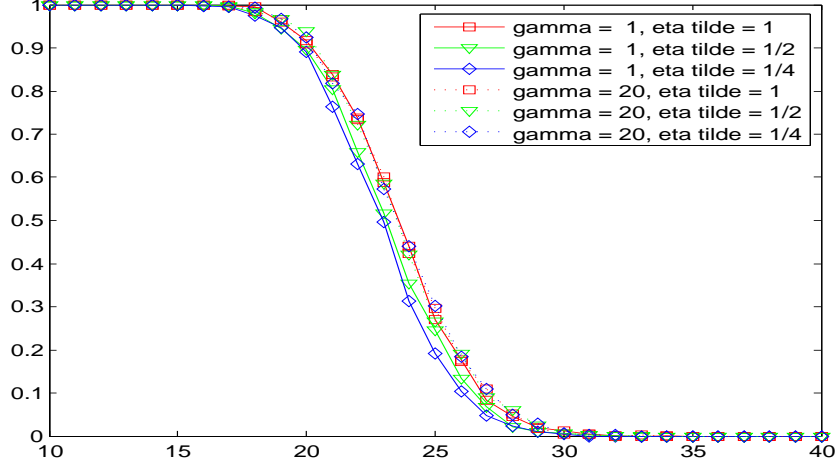


FIGURE 3. Success probabilities for Scheme II (a): $\eta = 1, \tilde{\eta} = 1, 1/2, 1/4$ with $\gamma = 1, 20$.

to see if the deviations from (21) have any impact on performance. Their probabilities of recovery are plotted as a function of the sparsity in Figure 2. Clearly, the performance deteriorates rapidly as the difference between the sampling and incident angles decreases. In other words, the backward scattering direction is the optimal sampling direction.

Likewise, to test Scheme II numerically, we use (23),

$$(32) \quad \tilde{\theta}_l = \phi_l + \frac{\tilde{\eta}\pi}{2} - \arcsin \frac{\rho_l}{\gamma\sqrt{2}}, \quad \tilde{\eta} = 1, 1/2, 1/4,$$

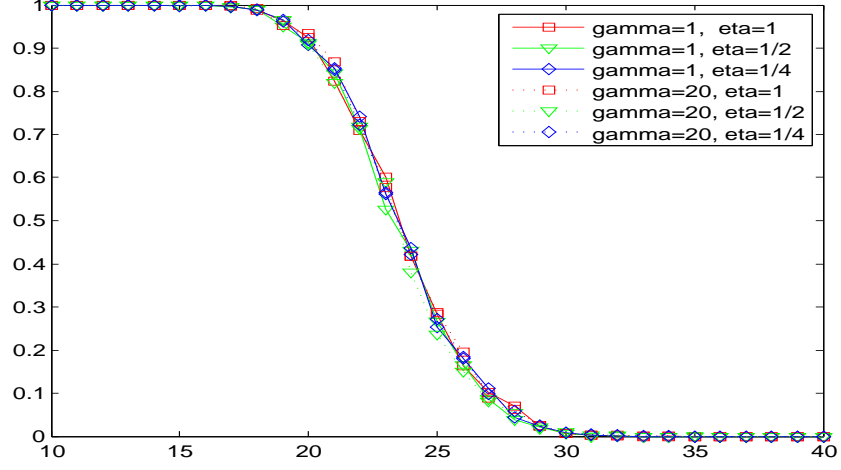


FIGURE 4. Success probabilities for Schemes II (b): $\eta = \tilde{\eta} = 1, 1/2, 1/4$ with $\gamma = 1, 20$.

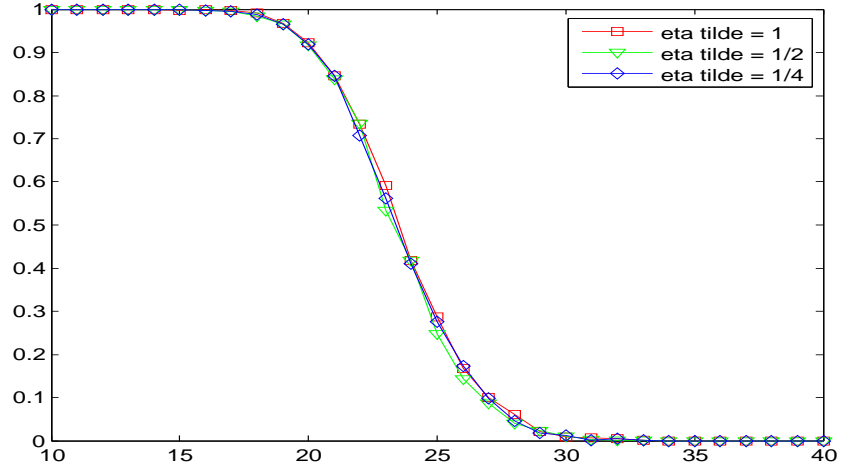


FIGURE 5. Success probabilities for Scheme III with (33).

and (24) with (a) $\eta = 1$ as well as (24) with (b) $\eta = \tilde{\eta} = 1, 1/2, 1/4$. Condition (26) is satisfied if and only if $\eta = \tilde{\eta}$.

The results for Case (a) at $\gamma = 1, 20$ are shown in Figure 3 and the results for Case (b) with $\eta = \tilde{\eta}$ at $\gamma = 1, 20$ are displayed in Figure 4. The slight degradation in performance for e.g., $\eta = 1, \tilde{\eta} = 1/4, \gamma = 1$ results from the violation of (26) whose validity is important for γ close to unity. For sufficiently large r , say $\gamma = 20$, the violation of (26) does not affect the performance (see below). On the other hand, when (26) holds, the performance is essentially independent of both γ and $\tilde{\eta}$, Figure 4.

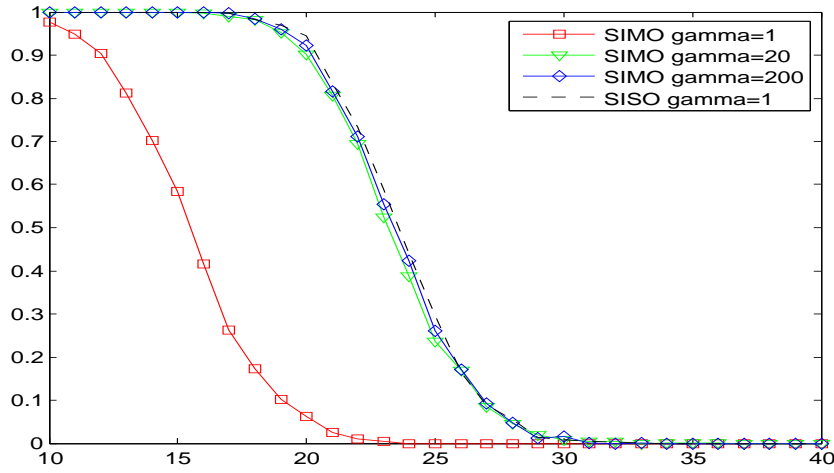


FIGURE 6. Solid curves are the success probabilities for the SIMO measurement at $\gamma = 1, 20, 200$ and the dashed curve is the SISO Scheme II at $\gamma = 1$.

For Scheme III we use equally spaced incident angles $\theta_l \in [\pi/6, \pi/3]$, (17) and

$$(33) \quad \theta_l + \tilde{\theta}_l = 2\phi_l + \tilde{\eta}\pi, \quad \tilde{\eta} = 1, 1/2, 1/4.$$

As shown in Figure 5, the performance is essentially independent of $\tilde{\eta}$.

Finally, we demonstrate numerically the SIMO schemes studied in [13] and compare their performance with that of the SISO schemes. A particular (one-shot) SIMO scheme relevant here would be to use (23) and (25) but for a fixed incident angle, say $\theta_l = 0, \forall l$ (In this case (26) is almost certainly violated). In [13] it is established that any SIMO scheme with independent sampling angles achieve a nearly optimal performance for a sufficiently high frequency (i.e. $\gamma \gg 1$). The success probabilities of the SIMO scheme for $\gamma = 1, 20, 200$ are calculated and plotted in Figure 6. Consistent with the theory [13], the low frequency case with $\gamma = 1$ has the worst performance. Clearly the performance of the one-shot SIMO scheme improves with γ and in the limit $\gamma \gg 1$ approaches that of the multiple-shot SISO Scheme II. There is negligible difference between the performances for $\gamma = 20$ and $\gamma = 200$ both of which follow closely that of the SISO Scheme II with $\gamma = 1$ (black dashed line in Figure 6).

4. CONCLUSION AND DISCUSSION

We have proposed, analyzed and numerically tested several SISO imaging schemes based on the RIP from theory of compressed sensing. Depending on the available frequencies, these schemes either multi-frequency band limited (I) or single frequency outside band (II). For Scheme I, the sampling direction is the backward direction while for Scheme II in the high frequency limit the optimal sampling direction is in the forward direction. In the case of point scatterers, both schemes produce nearly the same probability of recovery with the resolution given by (27), i.e.

$$\ell = \frac{\pi}{\sqrt{2}\Omega}$$

which is in line with the classical Rayleigh resolution criterion.

The SIMO schemes in which the scattered field of an incident angle is measured at multiple sampling angles have been studied in [13, 14, 15]. Except for the special case of the periodic scatterers lying on a transverse plane [14], it is not known if the sensing matrices of the SIMO schemes in general satisfy the RIP or not. In this case, the approach based on the notion of incoherence is taken to analyze the SIMO schemes [13, 15]. This approach is generally more flexible and should be applicable to the SISO schemes considered here.

The main advantage of the SIMO schemes is that in the one-shot setting (one incident field) the inverse scattering problem can be solved exactly *without* the Born approximation by inverting an auxiliary nonlinear system of equations [13]. We are working to extend the idea to the multiple-shot setting for both the SIMO and SISO schemes.

On the other hand, the SISO schemes with the RIP tend to have a better performance which can be matched by that of the SIMO schemes only at high frequency as demonstrated in Figure 6. The high frequency behavior of the SIMO schemes is analyzed in detail in [13].

Acknowledgement. I think my student Hsiao-Chieh Tseng for preparing the figures.

REFERENCES

- [1] M. Born and E. Wolf, *Principles of Optics*, 7-th edition, Cambridge University Press, 1999.
- [2] A.M. Bruckstein, D.L. Donoho and M. Elad, "From sparse solutions of systems of equations to sparse modeling of signals," *SIAM Rev.* **51** (2009), 34-81.
- [3] E. J. Candès, "The restricted isometry property and its implications for compressed sensing," *Compte Rendus de l'Academie des Sciences, Paris, Serie I.* **346** (2008) 589-592.
- [4] E. J. Candès, J. Romberg and T. Tao, "Robust uncertainty principles: Exact signal reconstruction from highly incomplete frequency information," *IEEE Trans. Inform. Theory* **52** (2006), 489-509.
- [5] E.J. Candès, J. Romberg and T. Tao, "Stable signal recovery from incomplete and inaccurate measurements," *Commun. Pure Appl. Math.* **59** (2006), 1207-1233.
- [6] E. J. Candès and T. Tao, "Decoding by linear programming," *IEEE Trans. Inform. Theory* **51** (2005), 4203-4215.
- [7] E. J. Candès and T. Tao, "Near-optimal signal recovery from random projections: universal encoding strategies?," *IEEE Trans. Inform. Theory* **52** (2006), 54-6-5425.
- [8] S.S. Chen, D.L. Donoho and M.A. Saunders, "Atomic decomposition by basis pursuit," *SIAM Rev.* **43** (2001), 129-159.
- [9] D. Colton and R. Kress, *Inverse Acoustic and Electromagnetic Scattering Theory*. 2nd edition, Springer, 1998.
- [10] W. Dai and O. Milenkovic, "Subspace pursuit for compressive sensing: closing the gap between performance and complexity," arXiv:0803.0811.
- [11] I. Daubechies, *Ten Lectures on Wavelets*. SIAM, Philadelphia, 1992.
- [12] D.L. Donoho and X. Huo, "Uncertainty principle and ideal atomic decomposition," *IEEE Trans. Inform. Theory* **47** (2001), 2845-2862.
- [13] A. Fannjiang, "Compressive inverse scattering I. High frequency SIMO measurements," arXiv: 0906.5405
- [14] A. Fannjiang, "Compressive imaging of subwavelength structures," arXiv:0905.3015.
- [15] A. Fannjiang, P. Yan and Thomas Strohmer, "Compressed remote sensing of sparse objects," arXiv:0904.3994
- [16] H. Rauhut, "Stability results for random sampling of sparse trigonometric polynomials," preprint, 2008.
- [17] M. Rudelson and R. Vershynin, "On sparse reconstruction from Fourier and Gaussian measurements," *Comm. Pure Appl. Math.* **111** (2008) 1025-1045.

E-mail address: fannjiang@math.ucdavis.edu

DEPARTMENT OF MATHEMATICS, UNIVERSITY OF CALIFORNIA, DAVIS, CA 95616-8633